SCIENTIFIC DATA

OPEN

Data Descriptor: Specific membrane capacitance, cytoplasm conductivity and instantaneous Young's modulus of single tumour cells

Ke Wang[1,2], Yang Zhao[1,3], Deyong Chen[1,2], Beiyuan Fan[1,2], Yulan Lu[1,2], Lianhong Chen[1,2], Rong Long[4], Junbo Wang[1,2] & Jian Chen[1,2]

As label-free biomarkers, biophysical properties of cells are widely used for cell type classification. However, intrinsic biophysical markers, e.g., specific membrane capacitance ($C_{specific\ membrane}$), cytoplasm conductivity ($\sigma_{conductivity}$) and instantaneous Young's modulus ($E_{instantaneous}$) measured for hundreds of single cells were not yet reported. In this study, single cells in suspension (adherent cells treated with trypsin) were aspirated through a microfluidic constriction channel at 25 °C, and the entry processes and impedance profiles were recorded and translated to $C_{specific\ membrane}$, $\sigma_{conductivity}$ and $E_{instantaneous}$. $C_{specific\ membrane}$, $\sigma_{conductivity}$ and $E_{instantaneous}$ of five cell types were quantified as $2.10 \pm 0.38\ \mu F\ cm^{-2}$, $0.91 \pm 0.15\ S\ m^{-1}$ and 5.52 ± 0.95 kPa for H460 cells ($n_{cell} = 437$); $2.52 \pm 0.54\ \mu F\ cm^{-2}$, $0.83 \pm 0.12\ S\ m^{-1}$ and 5.54 ± 1.04 kPa for H446 cells ($n_{cell} = 410$); $2.45 \pm 0.57\ \mu F\ cm^{-2}$, $0.99 \pm 0.18\ S\ m^{-1}$ and 5.16 ± 1.68 kPa for A549 cells ($n_{cell} = 442$); $1.86 \pm 0.31\ \mu F\ cm^{-2}$, $1.07 \pm 0.18\ S\ m^{-1}$ and 3.86 ± 0.81 kPa for 95D cells ($n_{cell} = 415$); $2.03 \pm 0.35\ \mu F\ cm^{-2}$, $0.99 \pm 0.16\ S\ m^{-1}$ and 3.49 ± 0.70 kPa for 95C cells ($n_{cell} = 290$). The database of $C_{specific\ membrane}$, $\sigma_{conductivity}$ and $E_{instantaneous}$ may serve as a reference for future studies of cellular biophysical properties.

Design Type(s)	cell type comparison design
Measurement Type(s)	Biophysical Chemistry
Technology Type(s)	microfluidics platform
Factor Type(s)	cancer cell line
Sample Characteristic(s)	H460 cell ● H446 cell ● A549 cell ● 95D cell ● 95C cell

[1]State Key Laboratory of Transducer Technology, Institute of Electronics, Chinese Academy of Sciences, Beijing 100190, PR China. [2]School of Electronic, Electrical and Communication Engineering, University of Chinese Academy of Sciences, Beijing 100190, PR China. [3]R&D Center for Healthcare Electronics, Institute of Microelectronics, Chinese Academy of Sciences, Beijing 100029, PR China. [4]Department of Mechanical Engineering, University of Colorado, Boulder, Colorado 80309, USA. Correspondence and requests for materials should be addressed to J.W. (email: jbwang@mail.ie.ac.cn) or to J.C. (email: chenjian@mail.ie.ac.cn).

Background & Summary

Biophysical properties of single cells include electrical parameters such as specific membrane capacitance ($C_{specific\ membrane}$, i.e., capacitance per unit area for the cell membrane modelled as a capacitor) and cytoplasm conductivity ($\sigma_{conductivity}$, i.e., the reciprocal of electrical resistivity or specific electrical resistance for the cytoplasm modelled as a resistor) as well as mechanical parameters such as instantaneous Young's modulus ($E_{instantaneous}$, which describes the initial elastic response of a cell, modelled as an incompressible viscoelastic solid, in response to mechanical forces), which are indicators of the status of cytoskeletons and cellular membranes[1]. Variations in cellular biophysical properties are closely related to physiological and pathological processes, examples including (1) red blood cells infected by malaria; (2) tumour cells during migration and evasion; (3) leukocytes affected by sepsis; and (4) stem cells undergoing differentiation[2,3].

Conventional techniques for characterizing the electrical properties of cells include patch clamping, electrorotation and dielectrophoresis[4–7]. On the other hand, atomic force microscopy, micropipette aspiration and optical tweezers have been used for characterizing the mechanical properties of cells[8–12]. Although well established, these approaches suffer from limited throughput (~1 cell per minute). In addition, they are not capable of measuring cellular electrical and mechanical properties simultaneously[1]. Therefore, data recording $C_{specific\ membrane}$, $\sigma_{conductivity}$ and $E_{instantaneous}$ for multiple cell types (hundreds of cells for each cell type) are currently not available in the literature.

Microfluidics is an area focusing on processing small amounts of fluids at the nanoliter to picoliter scale using microfabricated channels with dimensions of tens of micrometers[13–15]. The micrometer dimension is comparable to biological cells, and thus microfluidics is well suited for single-cell analysis[16,17]. More specifically, advances in microfluidic technology have enabled high-throughput characterization of the biophysical properties of single cells, e.g., through impedance flow cytometry, microfluidic optical stretchers and microfluidic hydrodynamic stretchers[1,8,18]. Although powerful, these previously reported microfluidics-based approaches only reported electrical (e.g., impedance flow cytometry) or mechanical (e.g., microfluidic optical stretchers and hydrodynamic stretchers) properties of single cells separately, without demonstrating simultaneous characterization of cellular electrical and mechanical properties.

Microfluidic approaches that enable simultaneous characterization of electrical and mechanical properties of single cells have also been developed, specifically through (1) microcantilever-based electrodes[19], (2) electrodeformation[20], (3) micropipette aspiration with impedance spectroscopy[21], or (4) constriction channels with impedance spectroscopy[22]. The first three approaches are limited by their low throughput, and thus cannot be used to collect data from hundreds of single cells. In the fourth approach, cells in suspension were aspirated through a constriction channel (with a width and a height that are smaller than the cell diameter) continuously. The deformation and impedance profiles of individual cells as they enter and travel through the constriction channel were recorded as mechanical and electrical signals, respectively, with an estimated throughput of 1 cell per second.

Based on custom-developed electromechanical models, these raw biophysical signals obtained from constriction channels with impedance spectroscopy were then translated to size-independent intrinsic biophysical markers including $C_{specific\ membrane}$, $\sigma_{conductivity}$ and $E_{instantaneous}$[23–25], enabling the classification of tumour cells with different malignant levels[26]. However, as proof-of-concept demonstrations, only a limited number of cell types were examined with small populations for each cell type[24].

In this study, based on the aforementioned approach, $C_{specific\ membrane}$, $\sigma_{conductivity}$ and $E_{instantaneous}$ from five types of tumour cells and hundreds of single cells for each cell type were quantified and reported. This study provides a preliminary database for cellular $C_{specific\ membrane}$, $\sigma_{conductivity}$ and $E_{instantaneous}$, which may serve as a reference for future studies on characterizing and classifying biological cells based on cellular biophysical properties.
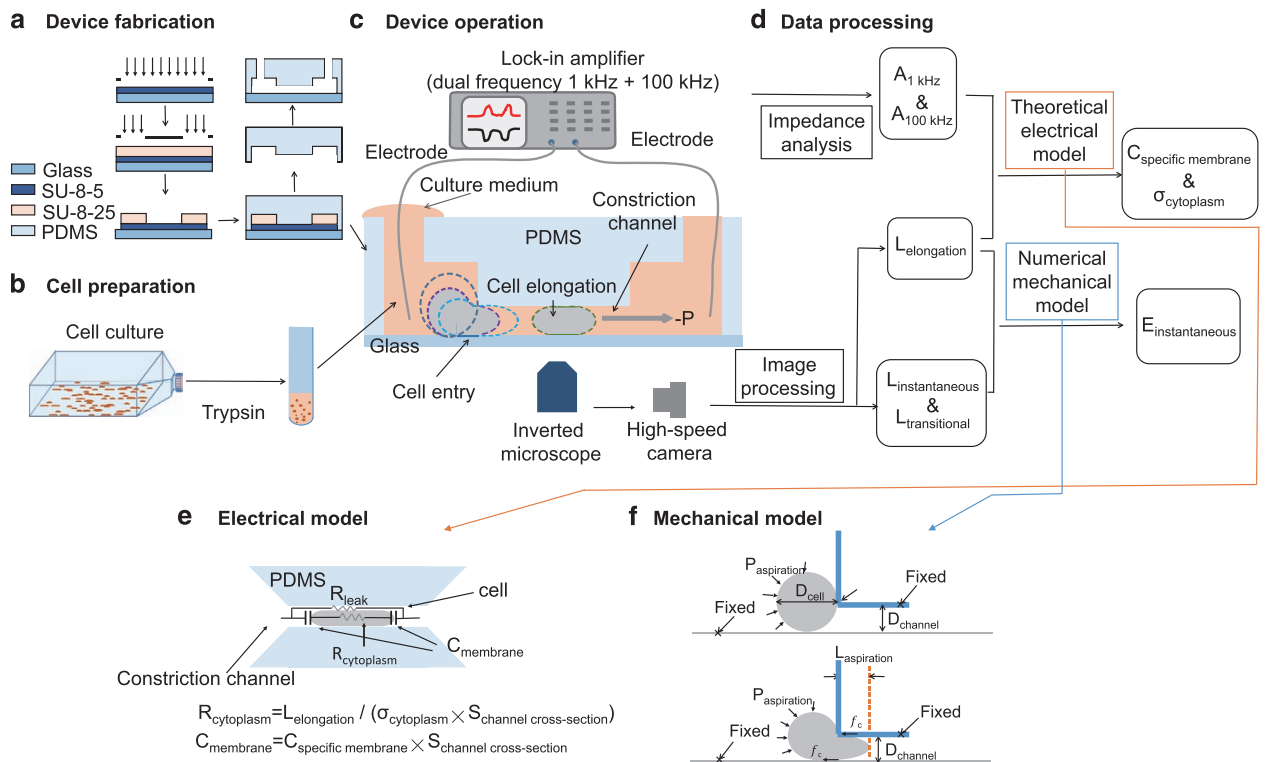
Methods

Working flowchart

The working flowchart for characterizing $C_{specific\ membrane}$, $\sigma_{conductivity}$ and $E_{instantaneous}$ includes four key steps: device fabrication, cell preparation, device operation and data processing (see Fig. 1). During operation, cells in suspension were aspirated into the microfluidic constriction channels with the deformation and impedance profiles of the cells recorded by a high-speed camera and an impedance analyser, respectively. Raw biophysical data were obtained by processing the images and impedance data captured in experiments, which were then translated to $C_{specific\ membrane}$, $\sigma_{conductivity}$ and $E_{instantaneous}$, based on a theoretical electrical model for a cell traveling within the constriction channel and a numerical mechanical model capturing the deformation of a cell when it enters the constriction channel, respectively. The key steps were summarized as follows. The detailed procedures have been reported in a previous publication[24].

Device fabrication

The microfluidic device consists of a constriction channel (a cross sectional area of $10\,\mu m \times 10\,\mu m$) in polydimethylsiloxane (PDMS) elastomer (Dow Corning Corp., Midland, MI, USA) which was replicated from a SU-8 (MicroChem Corp., Newton, MA, USA) mould master (see Fig. 1a).

Figure 1. Working flowchart for simultaneous characterization of $C_{specific\ membrane}$, $\sigma_{conductivity}$ and $E_{instantaneous}$ of single cells. Key steps include device fabrication (**a**), cell preparation (**b**), device operation (**c**) and data processing (**d**) leveraging developed electrical (**e**) and mechanical (**f**) models. During device operation, suspended cells were aspirated into the microfluidic constriction channels with the cell deformation and impedance profiles recorded by a high-speed camera and an impedance analyser, respectively. Preliminary biophysical markers including $A_{1\ kHz}$, $A_{100\ kHz}$, $L_{instantaneous}$, $L_{transitional}$ and $L_{elongation}$ were obtained based on processing of image and impedance data, which were then translated to $C_{specific\ membrane}$, $\sigma_{conductivity}$ and $E_{instantaneous}$, based on a theoretical electrical model for cells traveling within the constriction channel and a numerical mechanical model capturing cell deformation during the entry process, respectively.

Briefly, SU-8 5 was spun coated, prebaked and exposed without development and post exposure bake to form the layer of the constriction channel (10 µm in height). Then SU-8 25 was spin coated on top of the first SU-8 layer, exposed with alignment and developed, forming the cell loading channel with a height of 25 µm. PDMS precursor and curing agents (10:1 in weight) were mixed, poured on channel masters and baked for crosslinking. PDMS channels were then peeled away from the SU-8 masters, punched to form through holes as inlets and outlets, and bonded to glass slides after plasma treatment.

Cell preparation

All cell-culture reagents were purchased from Life Technologies Corporation (Carlsbad, CA, USA). The lung cancer cell lines of H460, H446, A549, 95D and 95C (China Infrastructure of Cell Line Resources, Beijing, China) were cultured at 37 °C in 5% CO_2 in RPMI 1640 medium (11875) supplemented with 10% heat-inactivated fetal bovine serum (10099), 100 units ml^{-1} penicillin and 100 µg ml^{-1} streptomycin (15140). Immediately prior to an experiment, cells were trypsinized (25200, 0.25% for 3 min) to form a solution of cell suspension at a concentration of 1×10^6 cells ml^{-1} (see Fig. 1b).

Device operation

During operation the device was first filled with culture medium and and a pipette was used to transfer the cell suspension solution to the entrance of the cell loading channel. A pressure calibrator (DPI-610 pressure calibrator, Druck, Billerica, MA, USA) was used to generate a negative pressure (0.5–1.2 kPa), aspirating cells continuously through the constriction channel with silver wires inserted into the inlet and the outlet of the device for impedance profile recording (see Fig. 1c).

An inverted microscope (IX71, Olympus Inc., Tokyo, Japan) in connection with a high-speed camera (M320S, Phantom Inc., Bublin, OH, USA) was used to capture the process of cellular entry and travelling in the constriction channel at 200 frames per second. Impedance data at both 1 and 100 kHz was measured by a lock-in amplifier (7270, Signal Recovery, Oak Ridge, TN, USA) with a sampling rate of
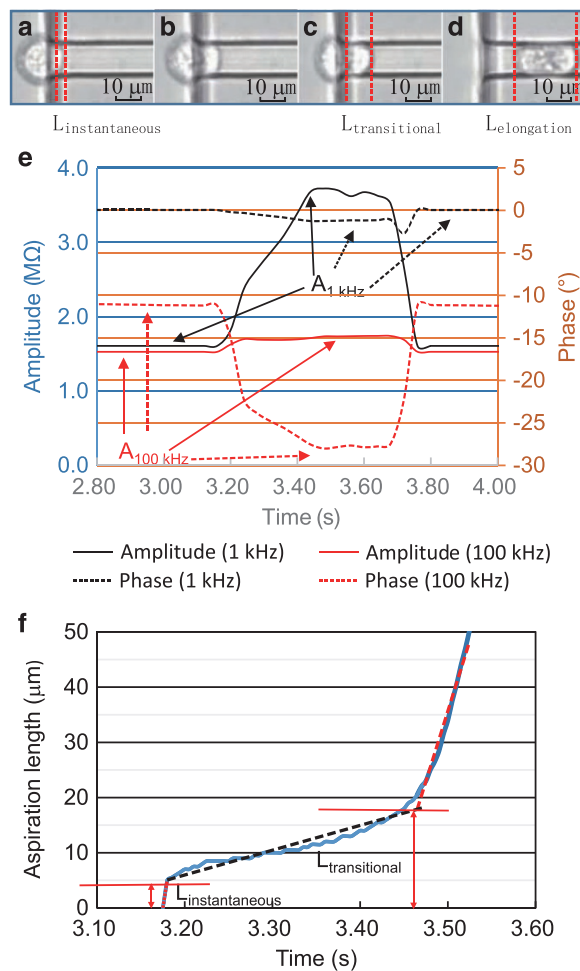
Figure 2. Raw imaging and impedance data for a typical cell to enter and travel in the constriction channel (length: 200 μm, width: 10 μm and height: 10 μm) with preliminary biophysical parameters quantified. (**a–d**) Microscopic pictures of a cell's entry and travelling process in the constriction channel with raw impedance data of the same cell shown in **e** and processed aspiration length versus time shown in **f**. Based on data processing, five preliminary biophysical parameters including $A_{1\text{ kHz}}$, $A_{100\text{ kHz}}$, $L_{instantaneous}$, $L_{transitional}$, and $L_{elongation}$ were obtained.

. . . .

25 points per second. All the characterization experiments were conducted within 30 min trypsinization of the cells at the room temperature (25 °C).

Data processing

At the stage when a cell enters the constriction channel, two preliminary parameters were quantified based on image processing: $L_{instantaneous}$ as the aspiration length when a cell instantaneously jumps into the channel and $L_{transitional}$ as the aspiration length at the point where the creep deformation of the cell ends (see Fig. 1d)[25]. During the stage when the cell is travelling within the constriction channel, the impedance profiles and images of the elongated cell were analysed which produced three preliminary parameters: $A_{1\text{ kHz}}$ and $A_{100\text{ kHz}}$, i.e., the ratios between the impedance amplitudes with and without a travelling cell at 1 and 100 kHz, respectively, as well as $L_{elongation}$, i.e., aspiration length of the cell when travelling within the constriction channel (see Fig. 1d)[23].

A theoretical model[23] was previously developed to model the electrical response of a cell as it is traveling within the constriction channel, thereby enabling the conversion of the measured $A_{1\text{ kHz}}$, $A_{100\text{ kHz}}$ and $L_{elongation}$ to $C_{specific\ membrane}$ and $\sigma_{conductivity}$ as size-independent intrinsic electrical markers for single cells. Briefly, the electrical response of a cell was represented by $R_{cytoplasm}$ and $C_{membrane}$ in series where R_{leak} indicated sealing properties during the cellular travelling process in the constriction channel. R_{leak} was derived from impedance data at 1 kHz ($A_{1\text{ kHz}}$) and $C_{membrane}$ and $R_{cytoplasm}$ were derived from impedance at 100 kHz ($A_{100\text{ kHz}}$), respectively, which, were further translated to $C_{specific\ membrane}$ and $\sigma_{cytoplasm}$ based on geometrical information of the constriction channel (see Fig. 1e). Note that in this study, the lumped electrical model was used for data interpretation where the membrane

portion was represented by $C_{membrane}$ and the cytoplasm portion was represented by $R_{cytoplasm}$, which, to an extent, neglects the potential effects of ion channels in the cell membrane and the membranes of cytosolic organelles in cytoplasm. Future studies may develop more accurate cellular electrical models.

On the other hand, a numerical mechanical model[25] was developed to model the cell deformation as it enters the constriction channel, where the channel walls were modelled as rigid surfaces and the cell was modelled as an incompressible viscoelastic solid. The key mechanical parameter to be extracted was $E_{instantaneous}$. Based on numerical simulations, the relationships between $L_{instantaneous}$, $L_{transitional}$ and $E_{instantaneous}$ were obtained as follows:

$$L_{ins\tan tan eous}/D_{channel} = \left(44.27f_c^2 - 37.24f_c + 13.70\right) \times P_{aspiration}/E_{ins\tan tan eous} + \left(-5.31f_c^2 + 2.84f_c - 0.59\right)$$
$$L_{transitional}/D_{channel} = \left(-60.40f_c^2 + 40.05f_c - 8.68\right) \times P_{aspiration}/E_{ins\tan tan eous} + \left(1.99f_c^2 + 0.03f_c + 1.60\right)$$

where $D_{channel}$ represents channel geometrical information, f_c represents the friction on cell-wall interfaces and $P_{aspiration}$ represents pressure applied to aspirate cells into the constriction channel (see Fig. 1f). The two unknown parameters, i.e., $E_{instantaneous}$ and f_c, were solved from these two equations since all the other parameters can be measured from experiments.

Data Records

Raw impedance and image data of five cell types are available at *Dryad repository* (Data Citation 1, Raw Impedance and Image Data of Single Tumour Cells). The file is an Excel composed of five sheets named after five cell lines of H460, H446, A549, 95D and 95C, respectively. In each sheet of a specific cell type, the first row is the cell number and within each cell number, there are seven columns which are time (collected from impedance analyser), amplitude at 1 kHz, phase at 1 kHz, amplitude at 100 kHz, phase at 100 kHz, time (collected from high-speed camera) and aspiration length.

$C_{specific\ membrane}$, $\sigma_{conductivity}$ and $E_{instantaneous}$ of five cell types are available at *Dryad repository* (Data Citation 1, Biophysical Properties of Single Tumour Cells). The file is an Excel composed of five sheets named after five cell lines of H460, H446, A549, 95D and 95C, respectively. In each sheet of a specific cell type, there are nine columns which are cell number (column A), $A_{1\ kHz}$ (column B), $A_{100\ kHz}$ (column C), $L_{instantaneous}$ (column D), $L_{transitional}$ (column E), $L_{elongation}$ (column F), $C_{specific\ membrane}$ (column G), $\sigma_{conductivity}$ (column H) and $E_{instantaneous}$ (column I). In this file, each row represents the biophysical parameters of a specific cell, including $A_{1\ kHz}$, $A_{100\ kHz}$, $L_{instantaneous}$, $L_{transitional}$, $L_{elongation}$, $C_{specific\ membrane}$, $\sigma_{conductivity}$ and $E_{instantaneous}$.

Technical Validation

Figure 2 shows a sequence of microscopic images (a–d), showing the entry process into the constriction channel for a single cell. In addition, the impedance data for the same cell was shown in Fig. 2e and the aspiration length as a function of time was obtained by image processing and shown in Fig. 2f. The detailed data for individual cells are included in (Data Citation 1, Raw Impedance and Image Data of Single Tumour Cells).

Based on the processing of impedance profiles and image processing, five preliminary biophysical markers of $A_{1\ kHz}$, $A_{100\ kHz}$, $L_{instantaneous}$, $L_{transitional}$, and $L_{elongation}$ were obtained. When the cell entered the constriction channel, an instantaneous jump into the constriction channel was initially observed (see Fig. 2a), enabling the quantification of $L_{instantaneous}$ in Fig. 2e. Then, a gradual increase in aspiration length (see Fig. 2b,e) was observed due to viscoelastic creep. The creep deformation ended when $L_{transitional}$ was reached (see Fig. 2c,e). Figure 2d shows an image of the cell travelling within the constriction channel where $L_{elongation}$ was quantified. Furthermore, impedance ratios at $A_{1\ kHz}$ and $A_{100\ kHz}$ were also quantified during the cellular travelling process in the constriction channel (see Fig. 2e). The averages and standard deviations of five preliminary biophysical markers ($A_{1\ kHz}$, $A_{100\ kHz}$, $L_{instantaneous}$, $L_{transitional}$ and $L_{elongation}$) for five types of tumour cells were summarized in Table 1. The detailed data for individual cells are included in (Data Citation 1, Biophysical Properties of Single Tumour Cells).

Cell Type	$A_{1\ kHz}$	$A_{100\ kHz}$	$L_{instantaneous}$ (μm)	$L_{transitional}$ (μm)	$L_{elongation}$ (μm)	$C_{specific\ membrane}$ (μF cm^{-2})	$\sigma_{cytoplasm}$ (S m^{-1})	$E_{instantaneous}$ (kPa)
H460 ($n_{celll} = 437$)	3.41 ± 0.47	1.17 ± 0.02	8.99 ± 1.15	18.14 ± 2.63	28.18 ± 2.42	2.10 ± 0.38	0.91 ± 0.15	5.52 ± 0.95
H446 ($n_{celll} = 410$)	2.94 ± 0.43	1.16 ± 0.03	9.20 ± 1.16	16.95 ± 1.55	28.29 ± 2.46	2.52 ± 0.54	0.83 ± 0.12	5.54 ± 1.04
A549 ($n_{celll} = 442$)	3.14 ± 0.56	1.14 ± 0.03	8.21 ± 1.48	17.31 ± 2.57	27.59 ± 3.66	2.45 ± 0.57	0.99 ± 0.18	5.16 ± 1.68
95D ($n_{celll} = 415$)	3.49 ± 0.49	1.17 ± 0.03	8.56 ± 1.01	17.68 ± 1.80	27.86 ± 2.34	1.86 ± 0.31	1.07 ± 0.18	3.86 ± 0.81
95C ($n_{celll} = 290$)	3.33 ± 0.43	1.19 ± 0.03	9.38 ± 1.21	19.06 ± 2.09	28.64 ± 2.31	2.03 ± 0.35	0.99 ± 0.16	3.49 ± 0.70

Table 1. A summary of biophysical parameters of five types of tumour cells. Five preliminary biophysical parameters (e.g., $A_{1\ kHz}$, $A_{100\ kHz}$, $L_{instantaneous}$, $L_{transitional}$ and $L_{elongation}$) and three size-independent intrinsic biophysical parameters (e.g., $C_{specific\ membrane}$, $\sigma_{cytoplasm}$ and $E_{instantaneous}$) were included.
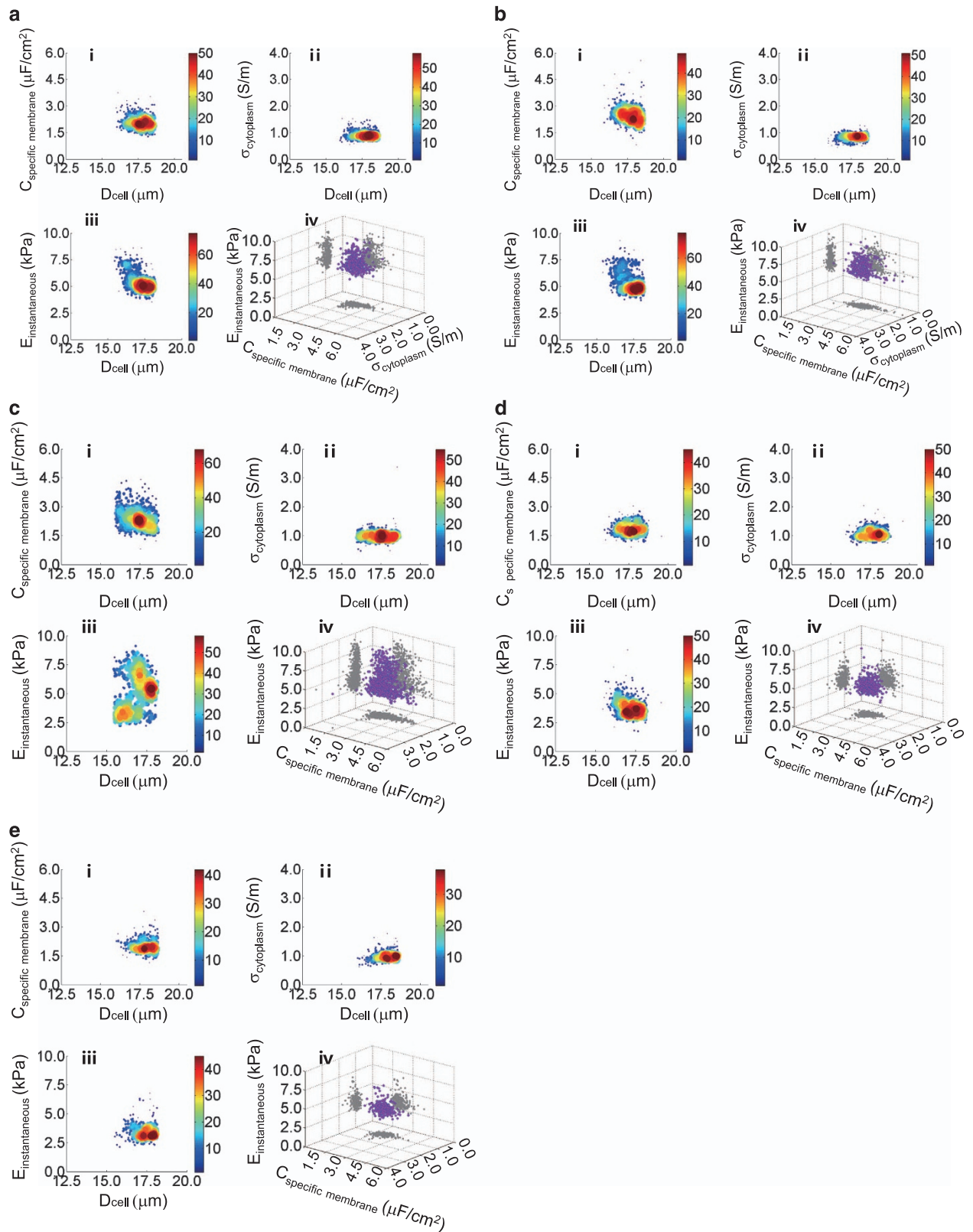
Figure 3. **Scatter plots of $C_{specific\ membrane}$, $\sigma_{conductivity}$ and $E_{instantaneous}$ of five tumour cells.** The number of measured cells for each type was 437 for H460 (**a**), 410 for H446 (**b**), 442 for A549 (**c**), 415 for 95D (**d**) and 290 for 95C cells (**e**). In addition, for each cell type, scatter plots of (i) $C_{specific\ membrane}$ versus D_{cell}, (ii) $\sigma_{conductivity}$ versus D_{cell}, (iii) $E_{instantaneous}$ versus D_{cell} and (iv) $C_{specific\ membrane}$ versus $\sigma_{conductivity}$ versus $E_{instantaneous}$ were included.

Figure 3a–e show the distributions of $C_{\text{specific membrane}}$, $\sigma_{\text{conductivity}}$ and $E_{\text{instantaneous}}$ for five types of tumour cells, respectively. For each type of tumour cells, the scatter plots of (i) $C_{\text{specific membrane}}$ versus D_{cell}, (ii) $\sigma_{\text{conductivity}}$ versus D_{cell}, (iii) $E_{\text{instantaneous}}$ versus D_{cell} and (iv) $C_{\text{specific membrane}}$ versus $\sigma_{\text{conductivity}}$ versus $E_{\text{instantaneous}}$ were included. Note that D_{cell} represents the diameter of the cell under measurement, which was calculated from $L_{\text{elongation}}$ based on the assumption of volume conservation when the cell deforms. As shown in Table 1, $C_{\text{specific membrane}}$, $\sigma_{\text{conductivity}}$ and $E_{\text{instantaneous}}$ of five cell types were found to be $2.10 \pm 0.38\,\mu\text{F cm}^{-2}$, $0.91 \pm 0.15\,\text{S m}^{-1}$ and $5.52 \pm 0.95\,\text{kPa}$ for H460 cells ($n_{\text{cell}} = 437$); $2.52 \pm 0.54\,\mu\text{F cm}^{-2}$, $0.83 \pm 0.12\,\text{S m}^{-1}$ and $5.54 \pm 1.04\,\text{kPa}$ for H446 cells ($n_{\text{cell}} = 410$); $2.45 \pm 0.57\,\mu\text{F cm}^{-2}$, $0.99 \pm 0.18\,\text{S m}^{-1}$ and $5.16 \pm 1.68\,\text{kPa}$ for A549 cells ($n_{\text{cell}} = 442$); $1.86 \pm 0.31\,\mu\text{F cm}^{-2}$, $1.07 \pm 0.18\,\text{S m}^{-1}$ and $3.86 \pm 0.81\,\text{kPa}$ for 95D cells ($n_{\text{cell}} = 415$); $2.03 \pm 0.35\,\mu\text{F cm}^{-2}$, $0.99 \pm 0.16\,\text{S m}^{-1}$ and $3.49 \pm 0.70\,\text{kPa}$ for 95C cells ($n_{\text{cell}} = 290$). The detailed data of $C_{\text{specific membrane}}$, $\sigma_{\text{conductivity}}$ and $E_{\text{instantaneous}}$ for individual cells are included in (Data Citation 1, Biophysical Properties of Single Tumour Cells).

References

1. Zheng, Y., Nguyen, J., Wei, Y. & Sun, Y. Recent advances in microfluidic techniques for single-cell biophysical characterization. *Lab on a Chip* **13**, 2464–2483 (2013).
2. Di Carlo, D. A mechanical biomarker of cell state in medicine. *Journal of Laboratory Automation* **17**, 32–42 (2012).
3. Suresh, S. Biomechanics and biophysics of cancer cells. *Acta Biomaterialia* **3**, 413–438 (2007).
4. Xu, Y. *et al.* A review of impedance measurements of whole cells. *Biosensors and Bioelectronics* **77**, 824–836 (2016).
5. Valero, A., Braschler, T. & Renaud, P. A unified approach to dielectric single cell analysis: impedance and dielectrophoretic force spectroscopy. *Lab on a Chip* **10**, 2216–2225 (2010).
6. Morgan, H., Sun, T., Holmes, D., Gawad, S. & Green, N. G. Single cell dielectric spectroscopy. *Journal of Physics D-Applied Physics* **40**, 61–70 (2007).
7. Gimsa, J., Stubbe, M. & Gimsa, U. A short tutorial contribution to impedance and AC-electrokinetic characterization and manipulation of cells and media: are electric methods more versatile than acoustic and laser methods? *Journal of Electrical Bioimpedance* **5**, 74–91 (2014).
8. Darling, E. M. & Carlo, D. D. High-throughput assessment of cellular mechanical properties. *Annual Review of Biomedical Engineering* **17**, 35–62 (2015).
9. Lim, C. T., Zhou, E. H., Li, A., Vedula, S. R. K. & Fu, H. X. Experimental techniques for single cell and single molecule biomechanics. *Materials Science and Engineering: C* **26**, 1278–1288 (2006).
10. Addae-Mensah, K. A. & Wikswo, J. P. Measurement techniques for cellular biomechanics *in vitro*. *Experimental biology and medicine* **233**, 792–809 (2008).
11. Lee, G. Y. H. & Lim, C. T. Biomechanics approaches to studying human diseases. *Trends Biotechnol* **25**, 111–118 (2007).
12. Helenius, J., Heisenberg, C. P., Gaub, H. E. & Muller, D. J. Single-cell force spectroscopy. *Journal of cell science* **121**, 1785–1791 (2008).
13. Wootton, R. C. & Demello, A. J. Microfluidics: Exploiting elephants in the room. *Nature* **464**, 839–840 (2010).
14. Whitesides, G. M. The origins and the future of microfluidics. *Nature* **442**, 368–373 (2006).
15. Squires, T. M. & Quake, S. R. Microfluidics: fluid physics at the nanoliter scale. *Reviews of Modern Physics* **77**, 977 (2005).
16. Sims, C. E. & Allbritton, N. L. Analysis of single mammalian cells on-chip. *Lab on a Chip* **7**, 423–440 (2007).
17. Reece, A. *et al.* Microfluidic techniques for high throughput single cell analysis. *Current Opinion in Biotechnology* **40**, 90–96 (2016).
18. Cheung, K. C. *et al.* Microfluidic impedance-based flow cytometry. *Cytometry A* **77**, 648–666 (2010).
19. Cho, Y. H., Yamamoto, T., Sakai, Y., Fujii, T. & Kim, B. Development of microfluidic device for electrical/physical character-ization of single cell. *Journal of Microelectromechanical Systems* **15**, 287–295 (2006).
20. MacQueen, L. A., Buschmann, M. D. & Wertheimer, M. R. Mechanical properties of mammalian cells in suspension measured by electro-deformation. *Journal of Micromechanics and Microengineering* **20**, 5007 (2010).
21. Chen, J. *et al.* A microfluidic device for simultaneous electrical and mechanical measurements on single cells. *Biomicrofluidics* **5**, 14113 (2011).
22. Zheng, Y., Shojaei-Baghini, E., Azad, A., Wang, C. & Sun, Y. High-throughput biophysical measurement of human red blood cells. *Lab on a Chip* **12**, 2560–2567 (2012).
23. Zhao, Y. *et al.* A microfluidic system enabling continuous characterization of specific membrane capacitance and cytoplasm conductivity of single cells in suspension. *Biosensors and Bioelectronics* **43C**, 304–307 (2013).
24. Zhao, Y. *et al.* Simultaneous characterization of instantaneous Young's modulus and specific membrane capacitance of single cells using a microfluidic system. *Sensors* **15**, 2763–2773 (2015).
25. Luo, Y. N. *et al.* A constriction channel based microfluidic system enabling continuous characterization of cellular instantaneous Young's modulus. *Sensors and Actuators B: Chemical* **202**, 1183–1189 (2014).
26. Zhao, Y. *et al.* Single-cell electrical phenotyping enabling the classification of mouse tumor samples. *Scientific reports* **6**, 19487 (2016).

Data Citation

1. Wang, K. *et al. Dryad Digital Repository* http://dx.doi.org/10.5061/dryad.3019k (2017).

Author Contributions

K.W., J.W. and J.C. designed experiments; K.W. and Y.Z. conducted experiments; B.F. conducted cell culture; K.W., Y.L. and L.C. processed experimental data; D.C. and R.L. developed electrical/mechanical models; K.W., R.L., J.W. and J.C. drafted the manuscript.

Additional Information

Competing financial interests: The authors declare no competing financial interests.

How to cite this article: Wang, K. *et al.* Specific membrane capacitance, cytoplasm conductivity and instantaneous Young's modulus of single tumour cells. *Sci. Data* 4:170015 doi: 10.1038/sdata.2017.15 (2017).

Publisher's note: Springer Nature remains neutral with regard to jurisdictional claims in published maps and institutional affiliations.